Mapping Impervious Cover Using Multi-Temporal MODIS NDVI Data

Joseph Knight and Margaret Voth

***Abstract*—Mapping impervious surfaces over regional or continental scale study areas with high spatial resolution imagery is difficult due to the cost and time involved in processing the large number of images required. This study investigated the benefits of using the coarse spatial resolution, high temporal resolution MODIS sensor to produce impervious surface maps. MODIS NDVI data for multiple years were analyzed with two multi-temporal image analysis methods: the Sequential Maximum Angle Convex Cone and Linear Spectral Unmixing. Impervious surface maps were generated and compared with a set of reference data and a Landsat-derived impervious cover map. The mapping accuracies for the algorithms used were generally good, particularly for the LSU approach, which was able to identify areas with 50–60% impervious cover at 77% accuracy and areas with a cumulative impervious cover of 50% or greater at 80% accuracy. The methods presented in this paper have potential for mapping impervious cover over large areas where the use of higher spatial resolution data is impracticable.**

***Index Terms*—Image processing, land cover, remote sensing.**

I. Introduction

LAND USE and Land Cover (LULC) maps derived from remotely sensed data are a valuable source of information about the status and trends of natural and anthropogenic impacts on the Earth. Multi-temporal remote sensing is proving to be a powerful tool for many assessment applications such as wetlands mapping [9], forest speciation [19], fire risk prediction [26], snow cover mapping [27], urban planning [6], and impervious surface mapping [5]. An important element drawn from LULC data is the amount of impervious surface present in an area. Impervious surface extents must be accounted for in many modeling applications, including hydrologic models of urban runoff and storm flow [13], [23], water quality monitoring [2], and studies of the urban heat island effect [1], [31].

Incorporating impervious surface estimates in regional or continental scale models is particularly challenging due to the tradeoff between the spatial resolution of the remotely sensed images used to map impervious surfaces and the cost and usability the resulting image data set. Landsat images have frequently been used to map impervious surfaces (e.g., [30]), but such imagery is difficult to acquire and process for large study areas. While not providing a comparable spatial resolution, the higher temporal resolution of the 250 meter MODIS sensor may allow for the computation of impervious surface estimates using sub-pixel information extraction [8]. This study evaluated the use of multi-temporal MODIS NDVI images to map impervious surfaces in a major metropolitan area.

Manuscript received October 31, 2009; revised January 11, 2010 and April 12, 2010; accepted May 07, 2010. Date of publication July 12, 2010; date of current version May 20, 2011. This work was supported in part by the University of Minnesota Graduate School, through the Grant in Aid Program.

The authors are with the Department of Forest Resources, University of Minnesota, St. Paul, MN 55119 USA (e-mail: jknight@umn.edu).

Digital Object Identifier 10.1109/JSTARS.2010.2051535

II. Study Area

This study was conducted in the Twin Cities Metropolitan Area (TCMA) of Minnesota, which surrounds the cities of Minneapolis and St. Paul and includes the counties of Anoka, Carver, Dakota, Hennepin, Ramsey, Scott, and Washington (Fig. 1). The TCMA is contained within the Temperate Deciduous Forest Biome, which is characterized by gently rolling topography, many lakes and rivers, a predominance of broadleaf deciduous trees such as oak and maple, and average annual values for temperature of 4–7 degrees Celsius, rainfall of 16–18 inches, and growing season of 100–130 days (Minnesota Department of Natural Resources [20]). The study area contains a wide variety of LULC types, including high density urban, suburban, urban fringe, forest, wetlands, and agriculture. The 7700 km^2 TCMA is dominated by the eponymous Twin Cities of Minneapolis and St. Paul, which have fueled significant population growth and urbanization in recent years. Between 1990 and 2000 the area's population grew by 16%, and from 2000 and 2007 the growth rate was 8% to 2.85 million people [18]. Such varied LULC types and rapid growth make the TCMA a suitable area for evaluating impervious surface mapping techniques.

III. Methods

Moderate Resolution Imaging Spectroradiometer (MODIS) Normalized Difference Vegetation Index (NDVI) data for 2004–2007 acquired by the National Aeronautics and Space Administration's (NASA) Terra satellite were obtained from the Warehouse Inventory Search Tool (WIST). These 250 meter spatial resolution NDVI datasets, referred to by the product name MOD13Q1, are created from BRDF corrected input images and provide a measure of the vegetative composition of each image pixel over a 16 day compositing period. The MOD13Q1 product is described as having approximately 0.5 pixel positional accuracy [21]. This accuracy estimate was confirmed in previous work [17]. In the research presented herein we have assumed that MODIS pixels represent the same ground area on each date. The NDVI values are influenced by vegetation type, amount, and vigor. A temporal profile of NDVI values is strongly representative of vegetation phenology, or interannual cycle.

This four year MODIS data set consisted of 92 individual images. The images were reprojected, clipped to the study area, and stacked using custom software. The stacked four year time

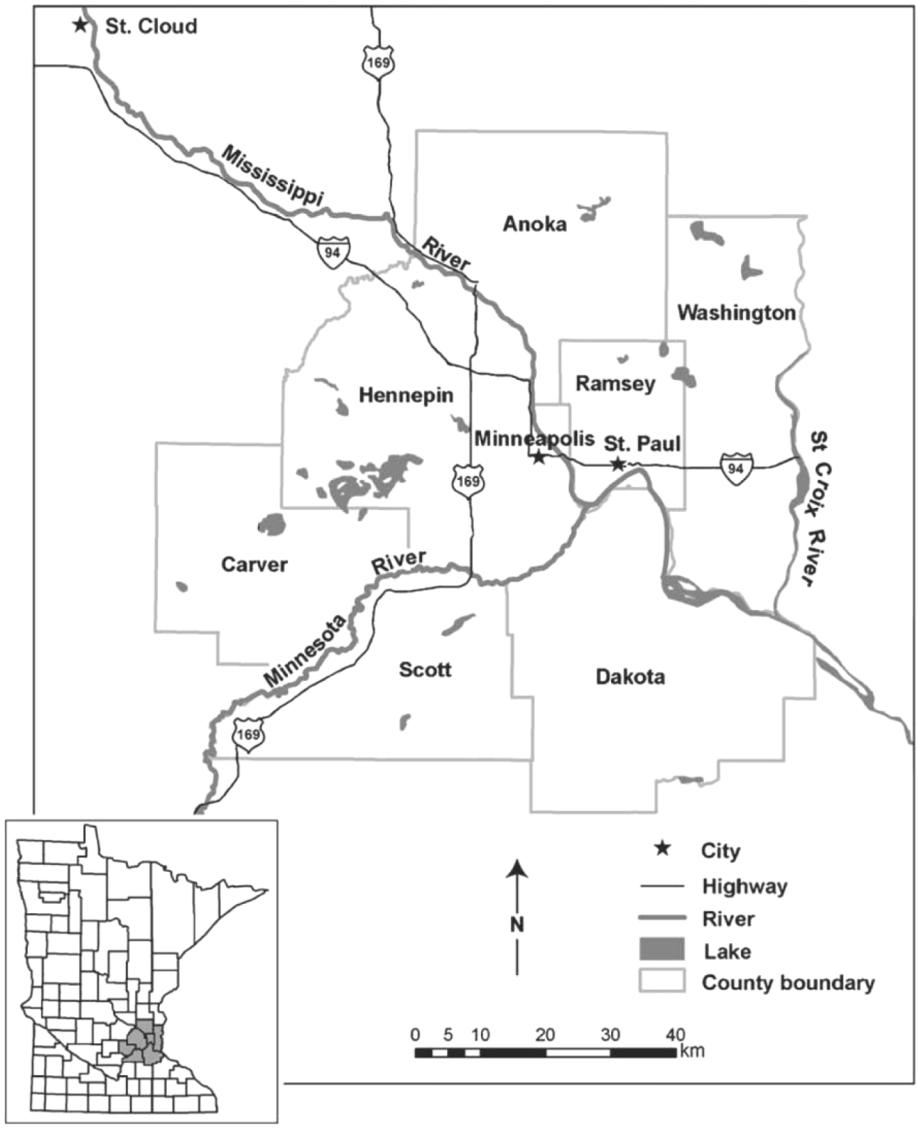

Fig. 1. The Twin Cities Metropolitan Area (figure by Yuan and Bauer [31], used with permission).

series data were then corrected using the Filter/Clean approach described in Lunetta *et al.* [17]. In brief, this process first examines the NASA-supplied MODIS Quality Assurance (QA) flags and removes pixel values with a QA level below "Acceptable." Next, obviously erroneous pixel values are removed. For example, if the NDVI value for a pixel drops significantly on one composite date and then returns to its previous value in the next date, the low value is assumed to be erroneous. Finally, new values for the removed low quality and erroneous pixels were interpolated using nonlinear deconvolution. The result of this process was a time series stack that more accurately represented the vegetation phenology signal present in each pixel. The cleaned MODIS NDVI time series was analyzed using four approaches: a simple band threshold, the SMACC algorithm, and Linear Spectral Unmixing applied to the full four year stack and a two year stack. Each of these methods is described below.

Band Threshold: Based on the assumption that pixels with relatively low NDVI values in the summer months would likely have some impervious surface composition, the MODIS NDVI image composite for July 14, 2005 was used to threshold the image. This date was chosen because it is typically near peak greenness in the TCMA and because the atmospheric conditions at that time were particularly good, allowing for confidence that the NDVI value recorded by MODIS are representative. An empirically determined NDVI value of 0.4 represented the threshold between high and low vegetation pixels. Areas with NDVI values less than or equal to 0.4 were set aside as likely to be partially or fully impervious. This method was intended to serve as a baseline for comparison with the more sophisticated multi-temporal techniques described below.

SMACC: A two year NDVI stack (2004–05 only) was analyzed using the Sequential Maximum Angle Convex Cone (SMACC) algorithm [11], [12]. SMACC is an endmember extraction algorithm typically used with hyperspectral data that works by identifying an initial image endmember and then sequentially finding additional endmembers that have maximally divergent spectral angles from existing endmembers. Ten image endmembers were extracted from the MODIS image stack.

The endmembers were assessed for their correspondence to *LC* classes of interest. One of the endmembers was found to be strongly representative of impervious surfaces. Nonzero values of this endmember were used to mask the study area into an impervious surface map.

Linear Spectral Unmixing (Two Years): The Linear Spectral Unmixing (LSU) algorithm treats each pixel as a linear combination of its constituent LULC classes, and that the relative contributions of each of those classes can be determined by "unmixing" the pixel using a spectral library containing "pure" examples of those LULC classes [22]. The normal work flow when using LSU with hyperspectral or multi-temporal data sets is to first perform a "whitening" procedure in which the noise signal present in the image is transformed to have unit variance and no band to band correlations [10], [4]. Algorithms typically used for noise whitening are Principal Components Analysis (PCA) and Minimum Noise Fraction (MNF) [14]. The coherent, theoretically noise free, bands produced by the whitening procedure are then used in further analyses such as LSU. Contrary to results reported by others (e.g., [15], [16], [24], [25], [29]), the use of noise whitening procedures on the TCMA NDVI data set resulted in a substantial decrease in impervious surface mapping accuracy. Therefore, the original unwhitened NDVI stack was used in the LSU analysis. It is likely that, in this case, the impervious surface signal was not distinct enough to be identified by the whitening algorithms as an important image component.

The spectral library used in the LSU analysis was composed of image endmember pixels identified manually as representing the cover types of interest. Initially, an attempt was made to select endmembers representing all of the LULC classes present in the study area, including impervious surface, agriculture, forests, water, etc. The performance of the LSU algorithm in identifying impervious surfaces using such a spectral library was unexpectedly poor. Simplifying the spectral library to include only the most distinct LULC classes greatly improved the mapping accuracy—so much so that the final library used in the LSU analysis contained only two endmembers: a pure impervious pixel and a pure deciduous forest pixel. The LSU algorithm therefore treated all of the image pixels as linear mixtures of impervious surface and vegetation exhibiting a strong phenological signal. The resulting endmember abundance maps show the fraction of impervious and vegetation for each pixel in the study area. The impervious endmember abundance map was used to produce the impervious surface maps described below.

Linear Spectral Unmixing (Four Years): The LSU experiment described above was repeated with four years of NDVI data, 2004–2007. The same image pixels were used to construct the four year spectral libraries as were used in the two year method. The purpose of repeating LSU with four years was to determine whether including additional temporal data would result in improved unmixing results.

Accuracy Assessment: Arguably the most important step in any LULC project is the creation of a reference data set with which to assess the accuracy of the maps produced [7]. A complicating factor in assessing the accuracy of a classification derived from 250 m image data was the disparity between the image pixel size and the average patch size of the landscape. Because the TCMA is quite heterogeneous at the 250 m scale, a reference data set that provided sub-pixel LULC information was required. In this study, the impervious surface mapping accuracy of each method was assessed using a reference data set created from 0.6 m color infrared aerial orthophotos acquired April 8, 13, and 14, 2005. The positional accuracy of these orthophotos is estimated to be 33.3 feet at 1:12 000 scale. For each of 1000 randomly selected MODIS pixels in the study area (Fig. 2), the areal percentages of twelve LULC classes, including impervious surface, were estimated using a 100 point dot grid superimposed upon the high resolution reference images. A trained analyst counted the number of dots appearing over each LULC class and recorded the values. To avoid inter-interpreter variation in these values, one analyst assessed all 1000 samples. This procedure provided sub-pixel LULC data for the reference MODIS pixels.

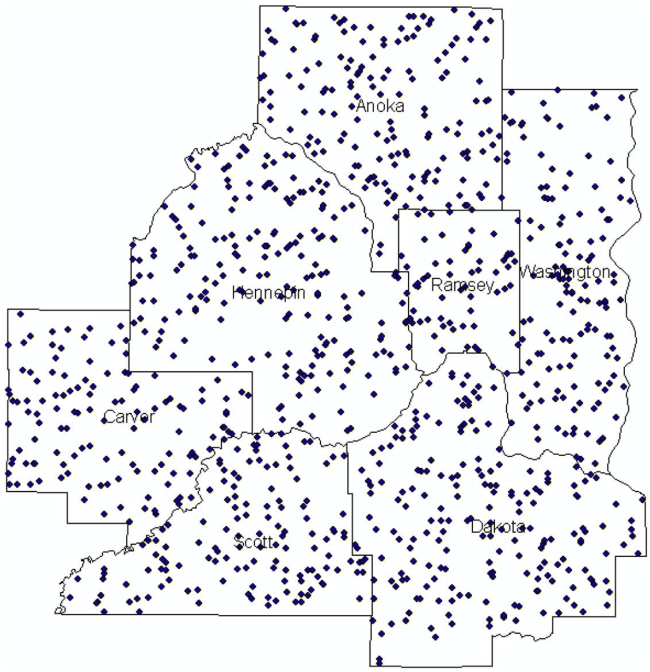

Fig. 2. Random reference sample distribution in the TCMA.

A separate validation of the impervious mapping results involved comparison with an impervious map derived from Landsat data by Yuan *et al.* [30]. The Landsat map was assessed using the reference dataset described above, with the Landsat map's mean pixel value compared with the 250 meter reference impervious percent value.

IV. Results and Discussion

The accuracy assessments results for the methods described above are presented in Tables I–VI. Impervious surface maps for each method are shown in Fig. 3. The accuracies of the impervious surface maps are presented in two ways: first, the accuracy in specified ranges of percent impervious surface as determined from the reference data (e.g., there were 10 reference pixels having impervious cover in the range of 71–80%), and second, the cumulative accuracy for impervious surface thresh-

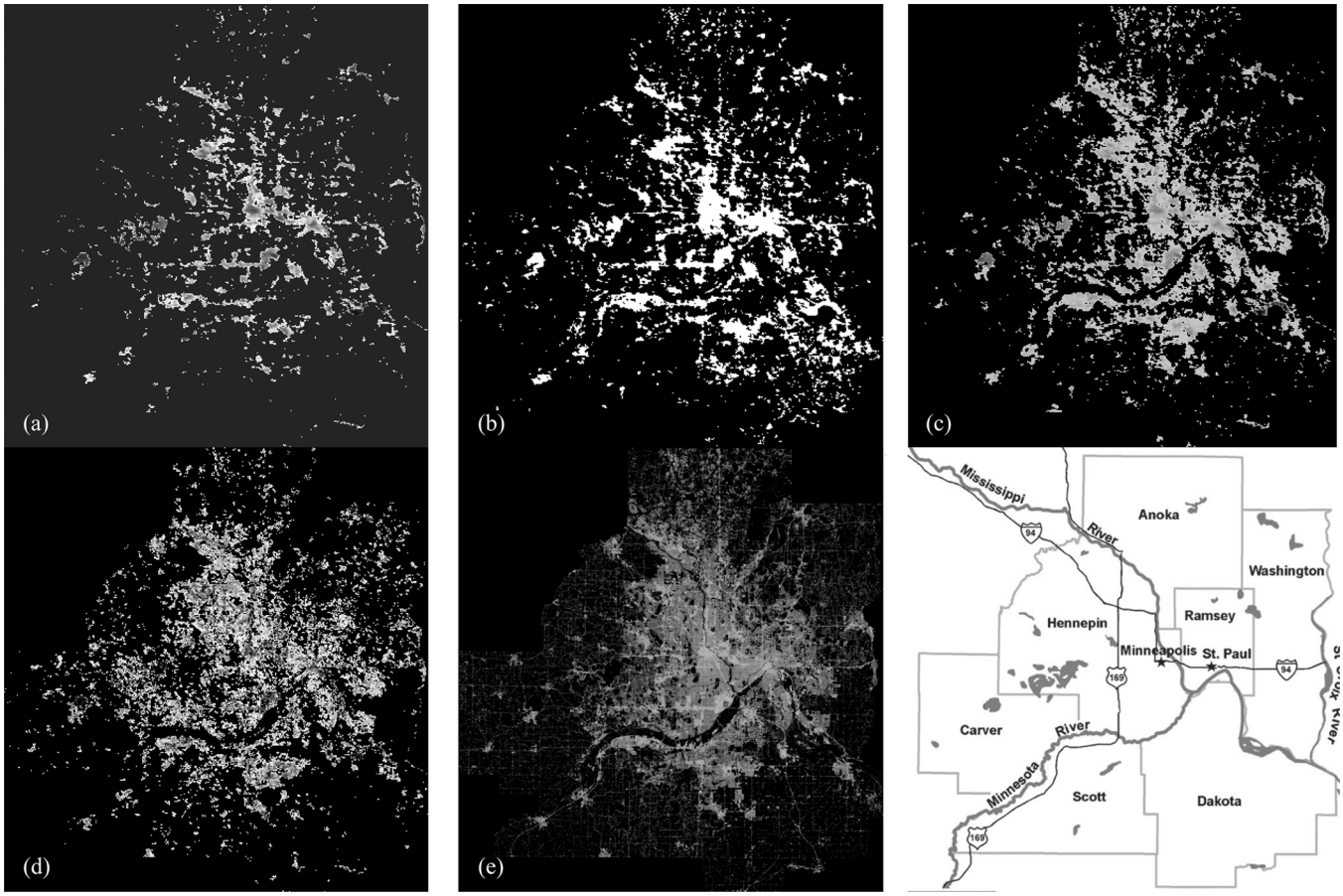

Fig. 3. (a) Impervious cover maps for band threshold. (b) SMACC, (c) four year LSU, (d) two year LSU, and (e) Landsat.

TABLE I
ACCURACY OF IMPERVIOUS SURFACE MAPPING: BAND THRESHOLD

Accuracy by Impervious % Ranges				Cumulative Accuracy			
%Imp	#Pts	#Imp	%Acc	%Imp	#Pts	#Imp	%Acc
>80%	8	7	88	>80%	8	8	100
71-80	10	8	80	>70%	18	16	89
61-70	18	10	56	>60%	36	26	72
51-60	43	16	37	>50%	79	42	53
41-50	61	15	25	>40%	140	57	41
31-40	75	11	15	>30%	215	68	32
21-30	75	4	5	>20%	290	72	25
1-20	397	5	1	>0%	687	77	11
0	313	0	100				

TABLE II
ACCURACY OF IMPERVIOUS SURFACE MAPPING: SMACC

Accuracy by Impervious % Ranges				Cumulative Accuracy			
%Imp	#Pts	#Imp	%Acc	%Imp	#Pts	#Imp	%Acc
>80%	8	8	100	>80%	8	8	100
71-80	10	9	90	>70%	18	17	94
61-70	18	15	83	>60%	36	32	90
51-60	43	22	51	>50%	79	54	68
41-50	61	24	39	>40%	140	78	56
31-40	75	20	27	>30%	215	98	46
21-30	75	14	19	>20%	290	112	39
1-20	397	23	6	>0%	687	135	20
0	313	10	96.8				

olds (e.g., there were 36 reference pixels having greater than 60% impervious cover).

The band threshold method (Table I) exhibited relatively poor performance. This method was able to identify pixels with a very high concentration of impervious surface but as the percent impervious cover decreased the accuracy dropped dramatically. Such a result was not unexpected, given the simplicity of the method, and serves to illustrate the usefulness of multi-temporal techniques. The band threshold map in Fig. 3(a) [as compared to the Landsat map in Fig. 3(e)] confirms that the threshold method identified only areas of relatively high impervious concentration such as the downtowns of Minneapolis and St. Paul and more developed surrounding areas.

The SMACC results are given in Table II. Like the band threshold method, the fully automated SMACC algorithm performed acceptably well when impervious concentrations were high but decreased in accuracy as percent impervious cover decreased. These results can be explained by the statistical underpinnings of the algorithm. The SMACC method is based on the Spectral Angle Mapper, which compares the angles formed between the automatically selected reference endmembers and the image pixel spectra, treating them as vectors in multidimensional space. As a correlative measure that does not distinguish between positive and negative correlations in the data, the SAM lacks the discriminatory power of algorithms such as LSU. Like the band threshold method, SMACC identified mainly areas of high impervious concentration, as is shown in Fig. 3(b).

The four year and two year LSU results are presented in Tables III and IV, respectively. The two approaches yielded nearly identical mapping accuracies, which suggests that two years of

TABLE III
ACCURACY OF IMPERVIOUS SURFACE MAPPING: 2004–2007 LSU

Accuracy by Impervious % Ranges				Cumulative Accuracy			
%Imp	#Pts	#Imp	%Acc	%Imp	#Pts	#Imp	%Acc
>80%	8	8	100	>80%	8	8	100
71-80	10	10	100	>70%	18	18	100
61-70	18	14	78	>60%	36	32	89
51-60	43	30	70	>50%	79	62	78
41-50	61	37	61	>40%	140	99	71
31-40	75	33	44	>30%	215	132	61
21-30	75	27	36	>20%	290	159	55
1-20	397	20	5	>0%	687	179	26
0	313	3	99				

TABLE IV
ACCURACY OF IMPERVIOUS SURFACE MAPPING: 2004–05 LSU

Accuracy by Impervious % Ranges				Cumulative Accuracy			
%Imp	#Pts	#Imp	%Acc	%Imp	#Pts	#Imp	%Acc
>80%	8	8	100	>80%	8	8	100
71-80	10	8	80	>70%	18	16	89
61-70	18	14	78	>60%	36	30	83
51-60	43	33	77	>50%	79	63	80
41-50	61	39	64	>40%	140	102	73
31-40	75	32	43	>30%	215	134	62
21-30	75	28	37	>20%	290	162	56
1-20	397	37	9	>0%	687	199	29
0	313	7	98				

TABLE V
ACCURACY OF IMPERVIOUS SURFACE MAPPING: LANDSAT (2002)

Accuracy by Impervious % Ranges				Cumulative Accuracy			
%Imp	#Pts	#Imp	%Acc	%Imp	#Pts	#Imp	%Acc
>80%	8	8	100	>80%	8	8	100
71-80	10	10	100	>70%	18	18	100
61-70	18	17	94	>60%	36	35	97
51-60	43	43	100	>50%	79	78	99
41-50	61	58	95	>40%	140	136	97
31-40	75	65	87	>30%	215	201	94
21-30	75	56	75	>20%	290	257	89
1-20	397	94	24	>0%	687	351	51
0	313	10	97				

data are enough to identify impervious surfaces with reasonable accuracy. The LSU results compare favorably with the band threshold and SMACC methods. LSU performance was similar to that of SMACC when impervious percent was low but was substantially better as imperviousness increased. The two year LSU's ability to identify areas with 50–60% impervious cover at 77% accuracy and areas with a cumulative impervious cover of 50% or greater at 80% accuracy is particularly notable. The two year LSU shown in Fig. 3(d) exhibits the best spatial agreement with the higher resolution Landsat map.

Table V shows the comparison of the Landsat-derived impervious cover map with the reference data. The Landsat map exhibited superior performance to all of the MODIS-derived maps across all of the impervious cover percentages. This result is due to Landsat's much higher spatial resolution and to the significant analyst input required to produce the map. It should be noted that the Landsat map was produced using 2002 images and was compared with 2005 reference data. It is therefore possible that the Landsat accuracy results presented were negatively impacted by change that occurred between 2002 and 2005.

TABLE VI
ACCURACY OF IMPERVIOUS SURFACE MAPPING: ALL METHODS

Percent Accuracy by Impervious % Ranges					
%Imp	SMACC	Diff	LSU4y	LSU2y	Landsat
>80%	100	88	100	100	100
71-80	90	80	100	80	100
61-70	83	56	78	78	94
51-60	51	37	70	77	100
41-50	39	25	61	64	95
31-40	27	15	44	43	87
21-30	19	5	36	37	75
1-20	6	1	5	9	24
0	96.8	100	99	98	97

Table VI summarizes the performance of the methods. All of the MODIS-derived algorithms performed well in areas with relatively high impervious cover. The increasingly subpar accuracy as percent imperviousness decreased is likely due to limitations imposed by the coarse spatial resolution of the MODIS sensor in discriminating mixed areas such as low density residential. Thus, while the commission errors of the algorithms are excellent, the omission errors may be unacceptable for use in some applications. Another limitation of this approach is the requirement of at least two years of MODIS data. Providing only a single year of images to the SMACC or LSU algorithms did not give good results. Thus, some LULC class conversions must have occurred in the study area during the two or four year image acquisition windows, which may impact the usability of the approach for applications needing very temporally granular LULC data.

An important consideration when using LSU to find impervious surfaces is that other cover types may have similar phenological profiles. For example, an area of bare soil or exposed rock will mimic the low annual NDVI response of an impervious surface. If such complications cause significant impacts on the usability of the approach, it may be possible to use spectral data in conjunction with the multi-temporal approach to discriminate confused classes. Another possible confusing factor is turbid water, which could have a steady low NDVI response. The use of a water mask made from MODIS or higher resolution data such as the NLCD may help to ameliorate such problems. Finally, the degree of tree cover in an area may affect the retrieval of impervious surface percentages. An older suburban area with significant tree cover may have a lower LSU-derived impervious estimate than the actual amount due trees overhanging impervious surfaces.

Tables VII and VIII show error matrices comparing both the LSU two year and Landsat classifications with the reference data impervious percentages. In terms of absolute accuracy, both methods performed poorly in identifying fine gradations in impervious surface composition. Each algorithm had a 40% overall accuracy rate, but the errors of omission and commission were quite different between them. The LSU algorithm substantially underestimated impervious cover at low impervious percentages (most likely due to the coarse spatial resolution of the MODIS sensor) and thus exhibited fewer errors of commission with respect to impervious. The Landsat method performed better at assigning some level of impervious cover

TABLE VII
ERROR MATRIX FOR LSU 2004–2005 IMPERVIOUS SURFACE PERCENTAGES

	Reference Data (% Impervious)										
Map	**0**	**1-20**	**21-30**	**31-40**	**41-50**	**51-60**	**61-70**	**71-80**	**>80**	**Tot**	**%Cor**
0	306	360	47	43	22	10	4	2		794	39
1-20	2	28	14	11	4	6	1			67	42
21-20	2	4	11	4	3	4	1			28	39
31-40	3	3	1	14	6	1	1	1		30	47
41-50		1		2	16	5	2	1		27	59
51-60			2		5	11	1			19	58
61-70		1			5	3	4	2		15	27
71-80						2	3	3		8	38
>80				1		1	1	1	8	12	67
Tot	313	397	75	75	61	43	18	10	8	1000	
%Cor	98	7	15	19	26	26	22	30	100		**40%**

TABLE VIII
ERROR MATRIX FOR LANDSAT IMPERVIOUS SURFACE PERCENTAGES

	Reference Data (% Impervious)										
Map	**0**	**1-20**	**21-30**	**31-40**	**41-50**	**51-60**	**61-70**	**71-80**	**>80**	**Tot**	**%Cor**
0	303	303	19	10	3	0	1	0	0	639	47
1-20	6	38	17	8	12	5	1	0	1	88	43
21-30	1	26	21	12	12	2	0	1	1	76	28
31-40		16	3	14	7	7	0	0	0	47	30
41-50	3	3	3	12	7	4	5	1	0	38	18
51-60		6	4	5	8	8	3	1	2	37	22
61-70		1	4	7	4	5	2	3	0	26	8
71-80		2	3	3	5	6	2	2	1	24	8
>80		2	1	4	3	6	4	2	3	25	12
Tot	313	397	75	75	61	43	18	10	8	1000	
%Cor	97	10	28	19	11	19	11	20	38		**40%**

to impervious-containing pixels but correspondingly exhibited more errors of commission. Both algorithms had high omission error rates. Of note is the performance of the LSU and Landsat methods in the producer's accuracies of the non-impervious pixels. These results suggest that neither algorithm is well suited for precise estimation of impervious surface cover, but may perform acceptably in deriving coarse estimates. Finally, both algorithms performed well in discriminating impervious from non-impervious cover—particularly if the definition of non-impervious is expanded to include 20% or less of such cover.

The accuracy assessment conducted in this study was based on a pixel by pixel comparison of the impervious surface maps with the reference data. Thus, the image pixels were assumed to represent the same area on the ground in each MODIS image and to align perfectly with the reference data source. Given the inherent positional uncertainties in geospatial data, it is likely that these assumptions were not always valid. However, visual inspection of the data indicated that impervious surface maps corresponded very well positionally with the reference data. The use of a minimum mapping unit (MMU) larger than one pixel, for example a 3×3 pixel block, could have lessened the effects of positional errors [7]. While the use of a MMU is recommended if impervious surface maps produced using the methods described herein are to be disseminated to the public, we view the pixel by pixel approach to be valid in the research context of this project.

V. CONCLUSION

We have presented multi-temporal impervious surface mapping methods that use the vegetation phenology signal derived from MODIS NDVI data. The LSU algorithm in particular performed well in identifying impervious versus non-impervious surfaces. While the Landsat-based mapping is superior in thematic accuracy, particularly at relatively low impervious concentrations, there are advantages to using MODIS NDVI data in study areas at a statewide, regional, or continental level. First, the MODIS scene size is much larger than that of higher spatial resolution sensors. The state of Minnesota is covered by one MODIS scene, while with Landsat several images would be required. Second, little preprocessing of the MODIS data is required, which saves analyst time. The NDVI data can be used after applying a relatively computationally inexpensive cleaning procedure, while Landsat data typically must be atmospherically corrected, georectified, and mosaicked. Third, the LSU mapping algorithm is simple and fast, requiring less than one minute to process the TCMA image stack. The amount of time required from data download completion to the production of a LSU-based impervious surface map can be as little as one hour. Finally, the thematic accuracy provided by the LSU approach could be suitable for applications in which higher resolution data availability, budget, or time are limiting factors.

ACKNOWLEDGMENT

The authors thank the two anonymous reviewers for their insightful and helpful comments.

REFERENCES

[1] C. Aniello, K. Morgan, A. Busbey, and L. Newland, "Mapping micro-urban heat islands using Landsat TM and a GIS," *Comput. Geosci.*, vol. 21, no. 8, pp. 965–967, 1995.

[2] C. A. Arnold, Jr. and C. J. Gibbons, "Impervious surface coverage: The emergence of a key urban environmental indicator," *J. American Planning Assoc.*, vol. 62, no. 2, pp. 243–258, 1996.

[3] J. W. Boardman and A. F. H. Goetz, "Sedimentary facies analysis using imaging spectrometry: A geophysical inverse problem," in *Proc. 3rd AVIRIS Workshop*, 1991, pp. 4–13, JPL Publication 91-28.

[4] J. W. Boardman and F. A. Kruse, "Automated spectral analysis: A geological example using AVIRIS data, north Grapevine Mountains, Nevada," in *Proc. ERIM 10th Thematic Conf. Geologic Remote Sensing*, Ann Arbor, MI, 1994, pp. 407–418.

[5] A. Chabaeva, D. L. Civco, and J. D. Hurd, "An assessment of impervious surface estimation techniques," *ASCE J. Hydrol. Eng.*, vol. 14, no. 4, pp. 377–387, 2009.

[6] D. L. Civco, J. D. Hurd, E. H. Wilson, C. L. Arnold, and S. Prisloe, "Quantifying and describing urbanizing landscapes in the northeast United States," *Photogramm. Eng. Remote Sens.*, vol. 68, no. 10, pp. 1083–1090, 2002.

[7] R. Congalton and K. Green, *Assessing the Accuracy of Remotely Sensed Data: Principles and Practices*. Boca Raton, FL: CRC/Lewis Press, 1999, p. 137.

[8] M. Flanagan and D. L. Civco, "Subpixel impervious surface mapping," in *Proc. 2001 ASPRS Annu. Conv.*, St. Louis, MO, 2001, p. 13.

[9] M. S. Gilmore, E. H. Wilson, N. Barrett, D. L. Civco, S. Prisloe, J. D. Hurd, and C. Chadwick, "Integrating multi-temporal spectral and structural information to map wetlands vegetation in a lower connecticut river tidal marsh," *Remote Sens. Environ.*, vol. 112, pp. 4048–4060, 2008.

[10] A. A. Green, M. Berman, P. Switzer, and M. D. Craig, "A transformation for ordering multispectral data in terms of image quality with implications for noise removal," *IEEE Trans. Geosci. Remote Sens.*, vol. 26, pp. 65–74, 1988.

[11] J. Gruninger, A. J. Ratkowski, and M. L. Hoke, "The sequential maximum angle convex cone (SMACC) endmember model," in *SPIE Proc., Algorithms for Multispectral, Hyperspectral and Ultraspectral Imagery*, Apr. 2004, vol. 5425-1.

[12] J. F. Knight and R. S. Lunetta, "Regional scale land cover characterization using MODIS NDVI 250 m multi-temporal imagery: A phenology-based approach," *Geosci. Remote Sens.*, vol. 43, no. 1, pp. 1–23, 2006.

[13] H. L. Lee and K. W. Bang, "Characterization of urban stormwater runoff," *Water Research*, vol. 34, no. 6, pp. 1773–1780, 2000.

[14] D. Lu and Q. Weng, "Spectral mixture analysis of the urban landscape in indianapolis with Landsat ETM+ imagery," *Photogramm. Eng. Remote Sens.*, vol. 70, no. 9, pp. 1053–1062, 2004.

[15] D. Lu, E. Moran, and M. Batistella, "Linear mixture model applied to Amazonian vegetation classification," *Remote Sens. Environ.*, vol. 87, pp. 456–469, 2003.

[16] D. Lu and Q. Weng, "Use of impervious surface in urban land-use classification," *Remote Sens. Environ.*, vol. 102, no. 1–2, pp. 146–160, 2006.

[17] R. S. Lunetta, J. F. Knight, J. Ediriwickrema, J. G. Lyon, and L. D. Worthy, "Land cover change detection using multi-temporal MODIS NDVI data," *Remote Sens. Environ.*, vol. 105, pp. 142–154, 2006.

[18] Twin Cities Regional Population. Metropolitan Council, Minneapolis/St. Paul, MN, 2009 [Online]. Available: http://www.metrocouncil.org/about/facts/TwinCitiesPopulationFacts.pdf, retrieved 10/27/09

[19] J. G. Mickelson, D. L. Civco, and J. A. Silander, Jr., "Delineating forest canopy species in the Northeastern United States using multi-temporal TM imagery," *Photogramm. Eng. Remote Sens.*, vol. 64, no. 9, pp. 891–904, 1998.

[20] Minnesota's Biomes Minnesota Dept. of Natural Resources, Minneapolis, MN [Online]. Available: http://www.dnr.state.mn.us/biomes/index.html, retrieved 10/28/09

[21] MOD13Q1. NASA, 2009 [Online]. Available: https://lpdaac.usgs.gov/lpdaac/products/modis_products_table/vegetation_indices/16_day_l3_global_250m/v5/terra, retrieved 10/29/09

[22] D. A. Roberts, M. Gardner, R. Church, S. Ustin, G. Scheer, and R. O. Green, "Mapping chaparral in the Santa Monica mountains using multiple endmember spectral mixture models," *Remote Sens. Environ.*, vol. 65, pp. 267–279, 1998.

[23] E. T. Slonecker, D. B. Jennings, and D. Garofalo, "Remote sensing of impervious surfaces: A review," *Remote Sens. Rev.*, vol. 20, no. 3, pp. 227–255, 2001.

[24] C. Small, "Estimation of urban vegetation abundance by spectral mixture analysis," *Int. J. Remote Sens.*, vol. 22, pp. 1305–1334, 2001.

[25] C. Small, "Multitemporal analysis of urban reflectance," *Remote Sens. Environ.*, vol. 81, pp. 427–442, 2002.

[26] J. Verbesselt, B. Somers, S. Lhermitte, I. Jonckheere, J. van Aardt, and P. Coppin, "Monitoring herbaceous fuel moisture content with SPOT VEGETATION time-series for fire risk prediction in savanna ecosystems," *Remote Sens. Environ.*, vol. 108, pp. 357–368, 2007.

[27] D. Vikhamar and R. Solberg, "Snow-cover mapping in forests by constrained linear spectral unmixing of MODIS data," *Remote Sens. Environ.*, vol. 88, pp. 309–323, 2003.

[28] E. H. Wilson, J. D. Hurd, D. L. Civco, S. Prisloe, and C. Arnold, "Development of a geospatial model to quantify, describe and map urban growth," *Remote Sens. Environ.*, vol. 86, no. 3, pp. 275–285, 2003.

[29] C. Wu and A. T. Murray, "Estimating impervious surface distribution by spectral mixture analysis," *Remote Sens. Environ.*, vol. 84, pp. 493–505, 2003.

[30] F. Yuan, K. E. Sawaya, B. C. Loeffelholz, and M. E. Bauer, "Land cover classification and change analysis of the twin cities (Minnesota) Metropolitan Area by multitemporal Landsat remote sensing," *Remote Sens. Environ.*, vol. 98, no. 2–3, pp. 317–328, 2005.

[31] F. Yuan and M. E. Bauer, "Comparison of impervious surface area and normalized difference vegetation index as indicators of surface heat island effects in Landsat imagery," *Remote Sens. Environ.*, vol. 106, no. 3, pp. 375–386, 2007.

Joseph Knight received the Ph.D. degree from North Carolina State University.

He is an Assistant Professor of geospatial science in the Department of Forest Resources, University of Minnesota, Twin Cities. He previously worked as a biologist with the United States Environmental Protection Agency.

Margaret Voth is a graduate student in the Natural Resources Science and Management program at the University of Minnesota.